Classical dispersion-cancellation interferometry

K.J. Resch[1,2], P. Puvanathasan[1], J.S. Lundeen[3], M.W. Mitchell[4], and K. Bizheva[1]

[1]*Department of Physics & Astronomy and* [2]*Institute for Quantum Computing, University of Waterloo, Waterloo, ON, Canada N2L 3G1*

[3]*Clarendon Laboratory, University of Oxford, Parks Rd, Oxford, United Kingdom OX1 3PU*

[4] *ICFO – Institut de Ciencies Fotoniques, Mediterranean Technology Park, 08860, Castelldefels (Barcelona), Spain*

kresch@iqc.ca

Abstract: Even-order dispersion cancellation, an effect previously identified with frequency-entangled photons, is demonstrated experimentally for the first time with a linear, classical interferometer. A combination of a broad bandwidth laser and a high resolution spectrometer was used to measure the intensity correlations between anti-correlated optical frequencies. Only 14% broadening of the correlation signal is observed when significant material dispersion, enough to broaden the regular interferogram by 4250%, is introduced into one arm of the interferometer.

OCIS codes: (270.0270) Quantum Optics; (260.3160) Interference; (260.2030) Dispersion

References and links

1. J. G. Fujimoto, M. E. Brezinski, G. J. Tearney, S. A. Boppart, B. Bouma, M. R. Hee, J. F. Southern, and E. A. Swanson, "Optical biopsy and imaging using optical coherence tomography," Nat. Med. **1**, 970-972 (1995).
2. A. F. Fercher, W. Drexler, C. K. Hitzenberger, and T. Lasser, "Optical coherence tomography - principles and applications," Rep. Prog. Phys. **66**, 239-303 (2003).
3. W. Drexler, "Ultrahigh resolution optical coherence tomography," J. Biomed. Opt. **9**, 47-74 (2004).
4. V. Giovannetti, S. Lloyd, and L. Maccone, "Quantum-enhanced measurements: beating the standard quantum limit," Science **306**, 1330-1336 (2004).
5. D. Leibfried, E. Knill, S. Seidelin, J. Britton, R. B. Blakestad, J. Chiaverini, D. B. Hume, W. M. Itano, J. D. Jost, C. Langer, R. Ozeri, R. Reichle, and D. J. Wineland, "Creation of a six-atom Schrödinger cat state," Nature **438**, 639-642 (2005).
6. C. K. Hong, Z. Y. Ou, and L. Mandel, "Measurement of subpicosecond time intervals between two photons by interference," Phys. Rev. Lett. **59**, 2044-2046 (1987).
7. A. M. Steinberg, P. G. Kwiat, and R. Y. Chiao, "Dispersion cancellation and high-resolution time measurements in a fourth-order optical interferometer," Phys. Rev. A **45**, 6659-6665 (1992).
8. A. M. Steinberg, P. G. Kwiat, and R. Y. Chiao, "Dispersion cancellation in a measurement of the single-photon propagation velocity in glass," Phys. Rev. Lett. **68**, 2421-2424 (1992).
9. J.D. Franson, "Nonlocal cancellation of dispersion," Phys. Rev. A **45**, 3126-3132 (1992).
10. A. F. Abouraddy, M. B. Nasr, B. E. A. Saleh, A. V. Sergienko, and M. C. Teich, "Quantum-optical coherence tomography with dispersion cancellation," Phys. Rev. A **65**, 053817 (2002).
11. M. B. Nasr, B. E. A. Saleh, A. V. Sergienko, and M. C. Teich , "Demonstration of dispersion-canceled Quantum-Optical Coherence Tomography," Phys. Rev. Lett. **91**, 083601 (2003).
12. B. I. Erkmen and J. H. Shapiro, "Phase-conjugate optical coherence tomography," Phys. Rev. A **74**, 041601, (2006).
13. A. F. Fercher, C. Hitzenberger, M. Sticker, R. Zawadzki, B. Karamata, and T.Lasser, "Numerical dispersion compensation for Partial Coherence Interferometry and Optical Coherence Tomography," Opt. Express **9**, 610-615 (2001), http://www.opticsinfobase.org/abstract.cfm?URI=oe-9-12-610

#83393 - $15.00 USD Received 24 May 2007; revised 26 Jun 2007; accepted 26 Jun 2007; published 28 Jun 2007

14. J. F. de Boer, C. E. Saxer, and J. S. Nelson, "Stable carrier generation and phase-resolved digital data processing in Optical Coherence Tomography," Appl. Opt. **40**, 5787-5790 (2001).
15. D. L. Marks, A. L. Oldenburg, J. J. Reynolds, and S. A. Boppart, "Autofocus algorithm for dispersion correction in Optical Coherence Tomography," Appl. Opt. **42**, 3038-3046 (2003).
16. M. Wojtkowski, V. Srinivasan, T. Ko, J. Fujimoto, A. Kowalczyk, and J. Duker, "Ultrahigh-resolution, high-speed, Fourier domain optical coherence tomography and methods for dispersion compensation Multimedia," Opt. Express **12**, 2404-2422 (2004). http://www.opticsinfobase.org/abstract.cfm?URI=oe-12-11-2404
17. K. Banaszek, A. S. Radunsky, and I. A. Walmsley, "Blind dispersion compensation for optical coherence tomography," Opt. Commun. **269**, 152-155 (2007).
18. R. S. Bennink, S. J. Bentley, and R. W. Boyd, " 'Two-Photon' Coincidence Imaging with a Classical Source," Phys. Rev. Lett. **89**, 113601 (2002).
19. F. Ferri, D. Magatti, A. Gatti, M. Bache, E. Brambilla, and L. A. Lugiato, "High-resolution ghost image and ghost diffraction experiments with thermal light," Phys. Rev. Lett. **94**, 183602 (2005).
20. K. J. Resch, K. L. Pregnell, R. Prevedel, A. Gilchrist, G. J. Pryde, J. L. OBrien, and A. G. White, "Time-reversal and super-resolving phase measurements," Phys. Rev. Lett. **98**, 223601 (2007).
21. R. Ghosh and L. Mandel, "Observation of nonclassical effects in the interference of two photons," Phys. Rev. Lett. **59**, 1903-1905 (1987).
22. G. Ghosh, "Sellmeier coefficients and dispersion of thermo-optic coefficients for some optical glasses," Appl. Opt. **36**, 1540-1546 (1997).

1. Introduction

Interferometry is an indispensable tool for precision measurements. Low-coherence, or white-light, interferometry is used for precise measurements of material properties, such as optical path length and dispersion. Optical coherence tomography (OCT), a technique for non-invasive medical imaging, is based on low-coherence interferometry [1, 2]. Both white light interferometry and OCT use broad bandwidth light sources to achieve micrometer scale image resolution [3]. Although large spectral bandwidth is essential for obtaining high resolution, it also increases dispersive broadening of the interferogram.

Quantum metrology uses quantum mechanical features, such as entanglement and squeezed light, to improve the sensitivity of measurement devices [4, 5]. A two-photon quantum interferometer [6], based on frequency-entangled photon pairs, has been demonstrated to be insensitive to all even orders of dispersion ([7, 8]; for a related, but distinct result, see [9]). This effect, known as quantum dispersion cancellation, was proposed as the basis for *quantum*-optical coherence tomography [10] and a proof-of-principle was demonstrated experimentally [11]. A very recent theoretical model [12] claims that interferometric dispersion cancellation does not require the use of individual pairs of entangled photons. The scheme is instead based on a nonlinear optical interferometer that employs broad-band phase conjugation between two reflections from the same sample. Experimental implementation of this technique would be extremely difficult requiring both development of novel optical sources and a suitable method of phase conjugation. Other approaches use numerical methods to compensate dispersion in data and images obtained with low-coherence interferometry or OCT [13, 14, 15, 16, 17].

Dispersion cancellation is staightforward in quantum interferometry, but the methods proposed so far in classical interferometry are not. Can we use the intuition derived from quantum technologies to achieve dispersion cancellation in a simpler way in a classical interferometer [18, 19, 20]? In this work, we show that dispersion cancellation can be achieved using only a classical light source, linear optics, and frequency-correlated detection. We review quantum dispersion cancellation and use its essentials to design an analogous classical system.

2. Theory

Consider the nonclassical two-photon interferometer shown in Fig. 1(a) [6]. The upper path is of length, L_1, and the lower path is of length, L_2=$L_1+\Delta$. A nonlinear crystal, pumped by a narrow bandwidth laser of frequency $2\omega_0$, generates photon pairs with central frequency ω_0, via

#83393 - $15.00 USD Received 24 May 2007; revised 26 Jun 2007; accepted 26 Jun 2007; published 28 Jun 2007

parametric down-conversion into the upper and lower paths of the interferometer in the state,

$$|\psi\rangle = \int d\delta\omega A(\omega_0+\delta\omega)|\omega_0+\delta\omega\rangle_1|\omega_0-\delta\omega\rangle_2, \tag{1}$$

The subscripts 1 and 2 are mode labels, and $A(\omega_0+\delta\omega)$ is the amplitude for a pair of photons of frequencies $\omega_0+\delta\omega$ in mode 1 and $\omega_0-\delta\omega$ in mode 2. The sum of the frequencies in each term of the superposition is fixed by energy conservation – this is a frequency-entangled state with perfect frequency anti-correlation. The photons are interferometrically combined at the 50/50 beamsplitter followed by two single-photon counting detectors. The signal of interest is the number of coincident photon detection events as a function of the optical delay, Δ.

Insertion of a dispersive, lossless medium of length, L, in the upper path of the interferometer results in a frequency-dependent phase shift, $\phi_M(\omega)$=$k_M(\omega)L$, where $k_M(\omega)$ is the wavevector at frequency, ω, in the material. We series expand $k_M(\omega)$ about ω_0:

$$k_M(\omega) \approx k(\omega_0) + \left.\frac{dk}{d\omega}\right|_{\omega_0}\delta\omega + \frac{1}{2}\left.\frac{d^2k}{d\omega^2}\right|_{\omega_0}\delta\omega^2 + ..., \tag{2}$$

The first derivative is the inverse of the group velocity, v_g, at ω_0 and leads to a shift in the centre of the interference pattern. The second derivative is the leading-order dispersive term, which causes loss of both spatial resolution and contrast in low-coherence interferometry by broadening the width and reducing the visibility of the interference pattern.

Following Ref.[7], we make the assumption $A(\omega_0+\delta\omega)$=$A(\omega_0-\delta\omega)$, i.e., the amplitude is symmetric about the central frequency ω_0. We find the expected coincidence rate, as a function of Δ is:

$$C(\Delta) \quad \propto \quad \int d\delta\omega\,|A(\omega_0+\delta\omega)|^2\left\{1-\cos\left[\frac{2\delta\omega(L+\Delta)}{c}-2L\frac{dk}{d\omega}\delta\omega\right]\right\}. \tag{3}$$

The expression is in agreement with Ref. [7], but uses slightly different notation. Notice that the second derivative does not appear – this is the dispersion cancellation. In fact, all higher-order even derivatives are cancelled. Maximum destructive interference occurs when the argument of the cosine term is zero for every frequency. This happens when the extra group delay imposed by the material is balanced by extra optical delay in the other arm of the interferometer. We will refer back to this expression when describing our classical system.

Now consider the Mach-Zehnder interferometer in Fig. 1(b). The dimensions and mode labels of this interferometer are identical to that described in Fig. 1(a), as is the dimension of the dispersive material; both beamsplitters are 50/50. The intensity spectrum of the input light is $I(\omega)$. The intensities registered by the spectrometers for a delay position, Δ, and frequency, ω, in the outputs labeled *a* and *b* are,

$$I_a(\omega,\Delta) \quad = \quad I(\omega)\cos^2\left[\frac{(\Delta+L)\frac{\omega}{c}-\phi_M(\omega)}{2}\right] \tag{4}$$

$$I_b(\omega,\Delta) \quad = \quad I(\omega)\sin^2\left[\frac{(\Delta+L)\frac{\omega}{c}-\phi_M(\omega)}{2}\right]. \tag{5}$$

Each of these intensities is affected by all orders of dispersion in the series expansion of $\phi_M(\omega)$.

Quantum dispersion cancellation is a result of frequency-entanglement in fourth-order, i.e., coincidence, detection. Our approach seeks to mimic this effect as closely as classical physics allows. We use frequency *correlations*, the classical analogue to entanglement, and measure a fourth-order signal, achieved by multiplying pairs of intensity measurements. Specifically, we

#83393 - $15.00 USD Received 24 May 2007; revised 26 Jun 2007; accepted 26 Jun 2007; published 28 Jun 2007

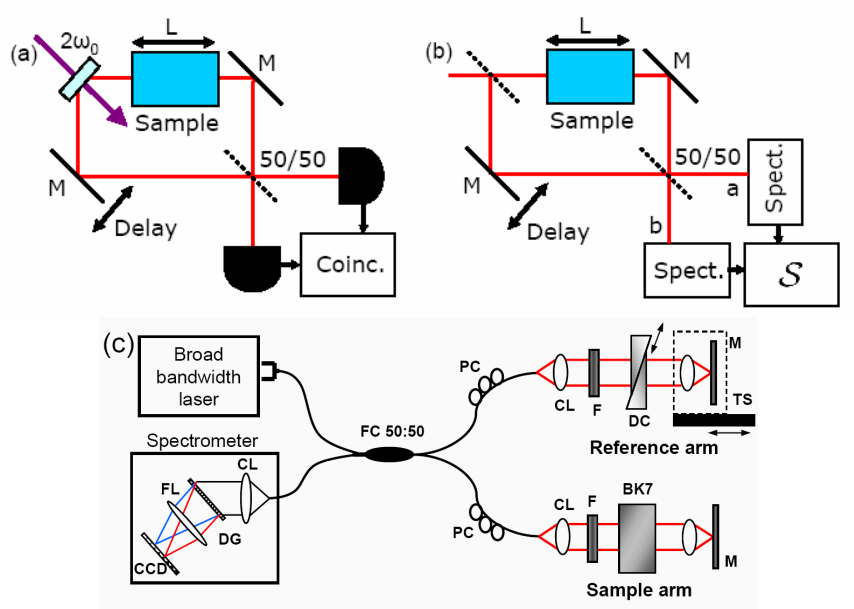

Fig. 1. Dispersion cancellation interferometry in a (a) Two-photon interferometer using frequency-entangled photon pairs [7, 8] and (b) a white-light Mach-Zehnder interferometer with frequency-correlated detection. These interferometers and their expected output signals are described in the text. Coinc. is coincidence detection; *S* describes a function of the output from the spectrometers. (c) Experimental realization. A broadband laser is the source for a fibre-based two-path (Michelson) interferometer. The setup uses a 50/50 beamsplitter (FC 50:50), polarization controllers (PC), collimating lenses (CL), neutral-density filters (F), two BK7 prisms for dispersion control (DC), a translation stage (TS), mirrors (M), and a spectrometer. The spectrometer contains a CL, a diffraction grating (DG), and focusing lens (FL).

measure the signal, S,

$$S(\Delta) \quad = \quad \int d\delta\omega I_a(\omega_0+\delta\omega)I_b(\omega_0-\delta\omega) \tag{6}$$

The integrand of this function is the product of two intensities with an energy sum of $2\omega_0$. We use Eq. (4) & Eq. (5) and assume, as we did in the quantum case, that the input spectrum is symmetric about ω_0, i.e., $I(\omega_0+\delta) = I(\omega_0-\delta)$, to obtain,

$$S(\Delta) \quad = \quad \frac{1}{2}\int d\delta\omega\,[I(\omega_0+\delta\omega)]^2 \left\{ \begin{array}{c} 1-\frac{1}{2}\cos\left[\frac{2\delta\omega(L+\Delta)}{c} - 2L\frac{dk}{d\omega}\delta\omega\right] \\ -\frac{1}{2}\cos\left[\frac{2\omega_0(L+\Delta)}{c} + 2Lk_0 + L\frac{d^2k}{d\omega^2}(\delta\omega)^2\right] \end{array} \right\} \tag{7}$$

This is the signal of interest from our classical system and can be directly compared with the quantum signal in Eq. (3). The argument in the first cosine term is identical to the quantum expression and describes a dispersion-cancelled interference dip. The second cosine term does not appear in the quantum case. Notice though, that its argument has only weak dependence on the frequency difference $\delta\omega$ (the integration variable) through the dispersion term. It describes a rapidly oscillating component, with wavelength $\lambda_0 = \pi c/\omega_0$, with a slowly decaying envelope. The separation of length-scales between these terms allows removal of the unwanted fast oscillation in the final data with for example, a low-pass Fourier filter. The other feature

#83393 - $15.00 USD Received 24 May 2007; revised 26 Jun 2007; accepted 26 Jun 2007; published 28 Jun 2007

of interest in our classical expression is that the first term is multiplied by 1/2. This imposes the well-known classical limit of 50% on the destructive interference visibility in two-photon interferometers [21, 6]. The signal, *S*, is the classical analogue to the Hong-Ou-Mandel dip [6] and contains the same resistance to dispersion as its quantum counterpart.

3. Experiment

The experimental setup is shown in Fig. 1(c). A compact, fiber-pigtailed, femtosecond laser (Femtolasers Inc., centre wavelength 792nm, bandwidth FWHM 154nm, average power 60mW) was coupled to a fiber-based Michelson interferometer. Broad bandwidth optical and fiber optic components were chosen to support propagation of the entire laser bandwidth with minimal spectral and power losses. A pair of BK7 prisms mounted on miniature translation stages in the reference arm of the system were used to precisely compensate material dispersion mismatch between the two arms of the interferometer. The focusing lens and the mirror in the reference arm of the system were mounted on a computer-controlled translation stage for variable optical delay. The interference pattern generated by light reflected from the sample and reference mirrors was detected with a high-resolution (0.09nm) and high-speed (20 kHz readout rate) spectrometer and recorded by a computer. The spectrometer utilized a 4096 pixel linear-array CCD camera and it was calibrated for the spectral range 607nm to 1012nm. To demonstrate dispersion cancellation with the classical interferometer, measurements were made both in a dispersion-balanced system and when flat, uncoated, BK7 optical windows of thickness 4.690 ± 0.005mm, 5.940 ± 0.005mm, and 6.170 ± 0.005mm (and several possible combinations) were introduced into the sample arm. For each measurement, the reference mirror was translated in steps of 0.1μm and the spectral interference fringes were acquired with a readout time of 60μs per step – at least 4 orders of magnitude shorter as compared with typical measurement times in entangled photon experiments.

The calculation of the signal function, *S*, was performed in the following way. One spectrometer reading was taken for each motor position to provide us with $I_a(\lambda,\Delta)$. The wavelength scale was converted to frequency and nonlinear interpolation was used to extract intensities at evenly spaced intervals. We obtained $I(\omega)$ by measuring the intensity from the sample and reference arm separately and doubling their sum. Energy conservation, $I(\omega)$=$I_a(\omega,\Delta)$+$I_b(\omega,\Delta)$, was applied to extract $I_b(\omega,\Delta)$ without the necessity for a second spectrometer. To satisfy the assumption in our theory that $I(\omega)$=$I(2\omega_0-\omega)$, $I(\omega)$ and $I_a(\omega)$ was multiplied by a mirror version of $I(\omega)$ with respect to the centre frequency ω_0. The integral *S* was approximated by a discrete sum over 4096 equally spaced energies.

4. Results and discussion

The total intensity registered by the spectrometer was obtained by summing the intensities measured at each pixel at a fixed translation stage position. This signal is equivalent to a signal that one would have been measured by a square-law detector, such as a photo-diode. Two examples of the total intensity measured as a function of the translation stage position are shown in Fig. 2 for the cases where no glass (a) and a 16.800 ± 0.009mm thick BK7 glass window (b) were inserted into the sample arm of the interferometer. Visibility is a measure of the contrast of interference. For oscillating interference, visibility is V_{osc}=$(I_{Max}-I_{Min})/(I_{Max}+I_{Min})$, where I_{Max} and I_{Min} are the maximum and minimum of the pattern. For interference dips the visibility we use the convention V_{dip}=$(I_{Max}-I_{Min})/I_{Max}$. As a result of the material dispersion, the intensity interference pattern is dramatically broadened, from $(2.04 \pm 0.03)\mu$m to $(88.6 \pm 0.9)\mu$m, and the fringe visibility is reduced, from 78% to 14%. These data clearly show the detrimental effect that dispersion has on interference.

The corresponding correlation signal function, *S*, for the two cases of no material dispersion

#83393 - $15.00 USD Received 24 May 2007; revised 26 Jun 2007; accepted 26 Jun 2007; published 28 Jun 2007

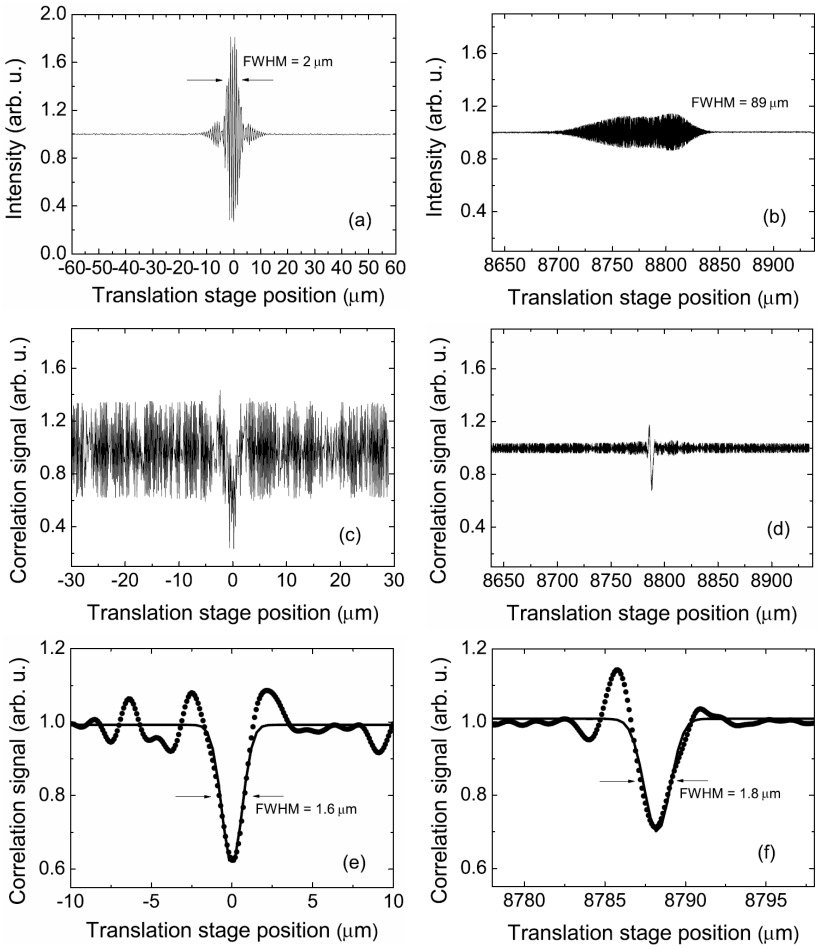

Fig. 2. Experimental Data. (a) & (b) Total intensity, as measured by summing the intensities measured at each frequency by the spectrometer, versus motor position with 0 and two passes through (16.800 ± 0.009)mm of BK7 glass in the sample arm of the interferometer, respectively. (c) & (d) *S* versus motor position with no BK7 and 16.8mm of BK7 in the sample arm. In (e) & (f), the data from (c) & (d) have been subject to a Fourier low-pass filter to remove rapidly oscillating terms. The solid curves are Gaussian fits. These data show that *S* broadens by only about 14% by addition of the glass while the standard intensity interference pattern is broadened by 4250%.

#83393 - $15.00 USD Received 24 May 2007; revised 26 Jun 2007; accepted 26 Jun 2007; published 28 Jun 2007

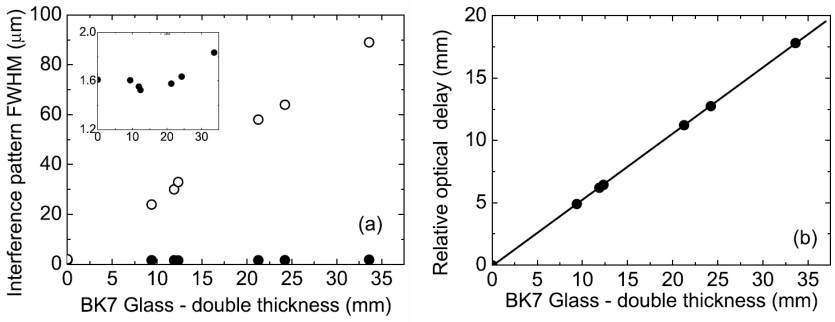

Fig. 3. Performance of classical dispersion cancellation. (a) The width of the interference patterns (total intensity, open circle; *S*, solid circle), as measured by translation stage displacement, versus the thickness of the glass traversed by the beam, i.e., twice the glass thickness. The inset expands the y-axis to show the almost constant width of *S* over the whole range of glass thicknesses. (b) The shift in the centre of the interference pattern versus the thickness of the glass. As discussed in the text, these data show that the interference pattern is displaced by the group delay.

and 16.800mm BK7 glass are shown in Fig. 2(c) and Fig. 2(d), respectively. Each of these signals has a sharp dip in addition to a rapidly oscillating component that corresponds to the final cosine term in Eq. (7). Note that the magnitude of the fast oscillating signal is *reduced* when a large amount of dispersion is present in the interferometer. A similar effect was observed when we simulated the measurements with a computer model. The data from Fig. 2(c) and Fig. 2(d) was filtered with a low-pass Fourier filter to remove the fast oscillating term and the the filtered data is presented in Fig. 2(e) and Fig. 2(f). These dips were fitted to a Gaussian function to extract their centres and FWHM. While the intensity interference pattern is broadened by 4250% of its original size due to material dispersion, the correlation signal *S* is broadened only by 14%. The visibility of the correlation signal dip is reduced from $(40.8 \pm 0.14)\%$ and $(30.0 \pm 0.3)\%$ for Fig. 2(e) and 2(f), respectively (recall that the theoretical maximum visibility is 50%). The deviations from the Gaussian shape of the fitting function are due partially to the non-Gaussian spectrum of the laser as well as the presence of higher-order material dispersion.

Figure 3(a) is a plot of the total intensity FWHM (open circles) and the correlation signal *S* FWHM (solid circles) as functions of twice the physical thickness of the BK7 optical flats (we use double the thickness because the Michelson interferometer uses a reflection geometry). The relative shift in the correlation signal dip centre as a function of twice the physical thickness of the glass in presented in Fig. 3(b). We estimated the statistical error in the centre of the dip to be about 1μm based on the standard deviation of 5 consecutive measurements. This is about a factor of 50-100 times larger than the fitting error and could be improved by using a higher precision translation stage. However, the most significant measurement error is associated with the widths of the BK7 flats. We expect the shift in the centre of the dip to be determined by the group velocity by the relation, $(c_{\text{air}}/v_g - 1)L$, where c_{air} is the speed of light in air and v_g is the group velocity, in our case at a wavelength of 800nm. From Fig. 3(b), we evaluate the slope 0.2633. The accepted value, 0.2631, was obtained from the Sellmeier equation [22]. Our errors are dominated by the uncertainty in the material thickness, which is about 0.1%, and at this level the slope from the data and the theory agree. The centre of the correlation signal *S* is determined by the group velocity.

#83393 - $15.00 USD Received 24 May 2007; revised 26 Jun 2007; accepted 26 Jun 2007; published 28 Jun 2007

5. Conclusion

We have theoretically derived and experimentally demonstrated a method for cancelling even-order dispersion in classical low-coherence interferometry. Dispersion cancellation is not a uniquely quantum effect, since it can also be observed in completely classical systems. However, the interference visibility in our classical analogue is only half that achievable in quantum interferometers [6, 8]. Two seemingly contradictory constraints are essential in both the quantum and classical techniques: a wide bandwidth of frequencies provides good time resolution, whereas narrow frequency correlations reduce sensitivity to dispersion. Our approach dramatically reduces experimental barriers for dispersion cancellation in low-coherence interferometry and optical coherence tomography.

6. Acknowledgments

We thank Aephraim Steinberg for valuable discussions and Gregor Weihs for loaning us equipment. This work was funded by the University of Waterloo, NSERC (KR,KB), and ORDCF (KB).

#83393 - $15.00 USD Received 24 May 2007; revised 26 Jun 2007; accepted 26 Jun 2007; published 28 Jun 2007